Inorg. Chem. **2006**, *45*, 8575–8583

Dilacunary Decatungstates Functionalized by Organometallic Ruthenium(II), $[\{Ru(C_6H_6)(H_2O)\}\{Ru(C_6H_6)\}(\gamma\text{-}XW_{10}O_{36})]^{4-}$ (X = Si, Ge)

Li-Hua Bi,[†] Elena V. Chubarova,[†] Nadeen H. Nsouli,[†] Michael H. Dickman,[†] Ulrich Kortz,*[,†] Bineta Keita,[‡] and Louis Nadjo*[,‡]

International University Bremen, School of Engineering and Science, P.O. Box 750 561, 28725 Bremen, Germany, and Laboratoire de Chimie Physique, UMR 8000, CNRS, Equipe d'Electrochimie et Photoélectrochimie, Université Paris-Sud, Bâtiment 420, 91405 Orsay Cedex, France

Received April 21, 2006

The benzene–Ru(II)-supported dilacunary decatungstosilicate $[\{Ru(C_6H_6)(H_2O)\}\{Ru(C_6H_6)\}(\gamma\text{-}SiW_{10}O_{36})]^{4-}$ and the isostructural decatungstogermanate $[\{Ru(C_6H_6)(H_2O)\}\{Ru(C_6H_6)\}(\gamma\text{-}GeW_{10}O_{36})]^{4-}$ have been synthesized and characterized by multinuclear solution NMR, IR, elemental analysis, and electrochemistry. Single-crystal X-ray analysis was carried out on $K_4[\{Ru(C_6H_6)(H_2O)\}\{Ru(C_6H_6)\}(\gamma\text{-}SiW_{10}O_{36})]\cdot 9H_2O$ (**K-1**), which crystallizes in the orthorhombic system, space group $Pmn2_1$, with $a = 13.6702(3)$ Å, $b = 16.2419(4)$ Å, $c = 12.1397(2)$ Å, and $Z = 2$, and on $K_4[\{Ru(C_6H_6)(H_2O)\}\{Ru(C_6H_6)\}(\gamma\text{-}GeW_{10}O_{36})]\cdot 7H_2O$ (**K-2**), which also crystallizes in the orthorhombic system, space group $Pmn2_1$, with $a = 13.6684(12)$ Å, $b = 16.297(2)$ Å, $c = 12.1607(13)$ Å, and $Z = 2$. Polyanions **1** and **2** consist of a $Ru(C_6H_6)(H_2O)$ group and a $Ru(C_6H_6)$ group linked to a dilacunary (γ-$XW_{10}O_{36}$) Keggin fragment resulting in an assembly with idealized C_s symmetry. The $Ru(C_6H_6)(H_2O)$ group is bound at the lacunary polyanion site via two Ru–O(W) bonds, whereas the $Ru(C_6H_6)$ group is bound on the side via three Ru–O(W) bonds. Polyanions **1** and **2** were synthesized in aqueous acidic medium at pH 2.5 by the reaction of $[Ru(C_6H_6)Cl_2]_2$ with $[\gamma\text{-}SiW_{10}O_{36}]^{8-}$ and $[\gamma\text{-}GeW_{10}O_{36}]^{8-}$, respectively. The formal potentials are roughly the same for the first W waves of **1** and **2**. However, important differences appear for the second W waves. These observations indicate different acid–base properties for the reduced forms of **1** and **2**. Three oxidation processes were detected: the oxidation of the Ru center is followed first by irreversible electrocatalytic processes of the Ru–benzene moiety and then of the electrolyte. Comparison of this behavior with that of the precursor reagent, $[Ru(C_6H_6)Cl_2]_2$, was useful to understand the main oxidation processes. A ligand substitution reaction was observed upon addition of dimethyl sulfoxide (dmso) to **1**, **2**, or $[Ru(C_6H_6)Cl_2]_2$. This reaction facilitates substantially the oxidation of the Ru center. The dmso was oxidized with large electrocatalytic currents more efficiently in the presence of **1** and **2** than with $[Ru(C_6H_6)Cl_2]_2$.

Introduction

Polyoxometalates are a unique class of inorganic molecules with nanomolecular dimensions. They exhibit an unmatched combination of useful and tunable properties including size, shape, composition, solubility, thermal and oxidative stability, and redox activity. Noble metal-substituted polyoxometalates (POMs) represent a subclass which is of fundamental and practical interest.[1] Very recently some examples of palladium-containing heteropolyanions have been reported by the groups of Hill and Kortz.[2] Ruthenium-containing POMs have also attracted considerable attention in the last couple

* To whom correspondence should be addressed. E-mail: u.kortz@iu-bremen.de (U.K.); louis.nadjo@lcp.u-psud.fr (L.N.). Fax: +49-421-200 3229 (U.K.).

[†] International University of Bremen.

[‡] Université Paris-Sud.

(1) (a) Pope, M. T. *Heteropoly and Isopoly Oxometalates*; Springer: Berlin, 1983. (b) Pope, M. T.; Müller, A. *Angew. Chem., Int. Ed. Engl.* **1991**, *30*, 34. (c) *Polyoxometalates: From Platonic Solids to Anti Retroviral Activity*; Pope, M. T., Müller, A., Eds.; Kluwer: Dordrecht, The Netherlands, 1994. (d) *Chem. Rev.* **1998**, *98*, 1−389 (Special Thematic Issue on Polyoxometalates). (e) *Polyoxometalate Chemistry: From Topology via Self-Assembly to Applications*; Pope, M. T., Müller A., Eds.; Kluwer: Dordrecht, The Netherlands, 2001. (f) *Polyoxometalate Chemistry for Nano-Composite Design*; Yamase, T., Pope, M. T., Eds.; Kluwer: Dordrecht, The Netherlands, 2002. (g) Pope, M. T. *Comput. Coord. Chem. II* **2003**, *4*, 635. (h) Hill, C. L. *Comput. Coord. Chem. II* **2003**, *4*, 679. (i) *Polyoxometalate Molecular Science*; Borrás-Almenar, J. J., Coronado, E., Müller, A., Pope, M. T., Eds.; Kluwer: Dordrecht, The Netherlands, 2004. (j) Casan-Pastor, N.; Gomez-Romero, P. *Front. Biosci.* **2004**, *9*, 1759.

10.1021/ic0606835 CCC: $33.50
Published on Web 09/16/2006

of years because of the unique catalytic properties of elemental ruthenium.[3] Therefore, Ru−POMs are highly interesting for redox applications[4] and, in particular, for the catalytic oxidation of organic substrates by O_2 and H_2O_2.[5] However, the number of structurally characterized, nonorganometallic ruthenium POMs is extremely small.[6] In addition, some of these Ru POMs are difficult to reproduce as stated in detail by Finke and Nomiya.[4a,7] Therefore, the search for novel well-characterized Ru POMs will add significant value to this research area.

The use of a clean, well-defined, soluble, cheap, and possibly air-stable Ru precursor appears to be key for the successful synthesis of ruthenium polyoxometalates. The tetra-dmso ruthenium(II) complex, *cis*-$Ru(dmso)_4Cl_2$, appears to fulfill essentially all these conditions. By using this precursor, our group was able to prepare three different Ru^{II}-$(dmso)_3$-supported polyoxotungstate structural types: $[HW_9O_{33}Ru_2(dmso)_6]^{7-}$, $[Ru(dmso)_3(H_2O)XW_{11}O_{39}]^{6-}$ (X = Ge, Si), and $[HXW_7O_{28}Ru(dmso)_3]^{6-}$ (X = P, As).[8]

Other examples of interesting Ru precursors are provided by the rich class of arene−Ru(II) species (arene = benzene, p-cymene, toluene, etc.). The group of Proust, especially, has successfully grafted a number of these organometallic fragments to different isopolymolybdates and -tungstates (e.g., $[\{Ru(\eta^6\text{-}p\text{-}MeC_6H_4iPr)\}_4W_4O_{16}]$ and $[\{Ru(\eta^6\text{-}C_6Me_6)\}_2Mo_5O_{18}\{Ru(\eta^6\text{-}C_6Me_6)(H_2O)\}]$) and lately also to lacunary phosphotungstates (e.g., $[\{PW_{11}O_{39}\{Ru(benzene)\}\}_2\{WO_2\}]^{8-}$) and a tungstoantimonate(III), $[Sb_2W_{20}O_{70}\{Ru(p\text{-cymene})\}_2]^{10-}$.[9−11] Very recently, we also started to work with the organometallic benzene−Ru(II) precursor $[Ru(C_6H_6)Cl_2]_2$. Reaction of this organo-ruthenium precursor with $[\alpha\text{-}XW_9O_{34}]^{10-}$ (X = Si, Ge) resulted in the di-$Ru^{II}(C_6H_6)$-supported $[(RuC_6H_6)_2XW_9O_{34}]^{6-}$ (X = Ge, Si).[12]

The dilacunary decatungstosilicate, $[\gamma\text{-}SiW_{10}O_{36}]^{8-}$, has been known for 20 years,[13] and since then, it has been widely used as a precursor in synthetic POM chemistry.[14] Mizuno and co-workers also studied the catalytic properties of $[\gamma\text{-}SiW_{10}O_{36}]^{8-}$, and they showed that it exhibits extremely high (99%) activity and selectivity in the epoxidation of olefins with hydrogen peroxide.[15] It is possible that grafting of organo-ruthenium(II) fragments onto the decatungstosilicate ion may generate synergistic effects which could result in even higher catalytic activity.

Here, we report on interaction of $[Ru(C_6H_6)Cl_2]_2$ with the dilacunary decatungstosilicate $[\gamma\text{-}SiW_{10}O_{36}]^{8-}$ and the very recently reported germanium analogue $[\gamma\text{-}GeW_{10}O_{36}]^{8-}$.[16]

Experimental Section

Synthesis. The polyanion precursors, $K_8[\gamma\text{-}SiW_{10}O_{36}]\cdot 12H_2O$ and $K_8[\gamma\text{-}GeW_{10}O_{36}]\cdot 6H_2O$, were synthesized according to the published procedures, and their purity was confirmed by infrared spectroscopy.[13,16] All other reagents were used as purchased without further purification.

$K_4[\{Ru(C_6H_6)(H_2O)\}\{Ru(C_6H_6)\}(\gamma\text{-}SiW_{10}O_{36})]\cdot 9H_2O$ (K-1). A 0.18 g (0.36 mmol) sample of $[Ru(C_6H_6)Cl_2]_2$ was dissolved in 20 mL of water, followed by the addition of 1.0 g (0.36 mmol) of $K_8[\gamma\text{-}SiW_{10}O_{36}]\cdot 12H_2O$. The pH value was adjusted to pH 2.5 by addition of 1 M HCl. This solution was heated to 80 °C for 1 h and then cooled to room temperature. The solution was filtered, and then 2.0 mL of 1.0 M KCl was added. This solution was allowed to evaporate in an open beaker at room temperature. A yellow crystalline product started to appear after about 3 days. Evaporation was continued until the solvent approached the solid product (yield = 0.36 g, 32%). IR of **K-1**: 3083(w), 2923(w), 2851(w), 2360(w), 2339(w), 1435(m), 1152(w), 992(m), 948(s), 904(sh), 881(sh), 868(s), 776(s), 752(s), 685(m), 614(w), 558(m), 498(w), 473(w) cm^{-1}. Anal. Calcd (Found) for **K-1**: K, 5.0 (5.2);

(2) (a) Anderson, T. M.; Neiwert, W. A.; Kirk, M. L.; Piccoli, P. M. B.; Schultz, A. J.; Koetzle, T. F.; Musaev, D. G.; Morokuma, K.; Cao, R.; Hill, C. L. *Science* **2004**, *306*, 2074. (b) Anderson, T. M.; Cao, R.; Slonkina, E.; Hedman, B.; Hodgson, K. O.; Hardcastle, K. I.; Neiwert, W. A.; Wu, S. X.; Kirk, M. L.; Knottenbelt, S.; Depperman, E. C.; Keita, B.; Nadjo, L.; Musaev, D. G.; Morokuma, K.; Hill, C. L. *J. Am. Chem. Soc.* **2005**, *127*, 11948. (c) Bi, L.-H.; Kortz, U.; Keita, B.; Nadjo, L.; Daniels, L. *Eur. J. Inorg. Chem.* **2005**, 3034. (d) Bi, L.-H.; Kortz, U.; Keita, B.; Nadjo, L.; Borrmann, H. *Inorg. Chem.* **2004**, *43*, 8367. (e) Bi, L.-H.; Reicke, M.; Kortz, U.; Keita, B.; Nadjo, L.; Clark, R. J. *Inorg. Chem.* **2004**, *43*, 3915. (f) Angus-Dunne, S. J.; Burns, R. C.; Craig, D. C.; Lawrance, G. A. *J. Chem. Soc., Chem. Commun.* **1994**, 523.

(3) (a) Naota, T.; Takaya, H.; Murahashi, S.-I. *Chem. Rev.* **1998**, *98*, 2599. (b) *Ruthenium in Organic Synthesis*; Murahashi, S.-I., Ed.; Wiley: New York, 2004.

(4) (a) Finke, R. G.; Yin, C. X. *Inorg. Chem.* **2005**, *44*, 4175. (b) Matsumoto, Y.; Asami, M.; Hashimoto, M.; Misono, M. *J. Mol. Catal. A: Chem.* **1996**, *114*, 161. (c) Hill, C. L.; Prosser-McCartha, C. M. *Coord. Chem. Rev.* **1995**, *143*, 407. (d) Bart, J. C.; Anson, F. C. *J. Electroanal. Chem.* **1995**, *390*, 11.

(5) (a) Neumann, R.; Dahan, M. *J. Am. Chem. Soc.* **1998**, *120*, 11969. (b) Neumann, R.; Dahan, M. *Polyhedron* **1998**, *17*, 3557. (c) Neumann, R.; Dahan, M. *Nature* **1997**, *388*, 353. (d) Neumann, R.; Khenkin, A. M.; Dahan, M. *Angew. Chem., Int. Ed. Engl.* **1995**, *34*, 1587.

(6) (a) Randall, W. J.; Weakley, T. J. R.; Finke, R. G. *Inorg. Chem.* **1993**, *32*, 2, 1068. (b) Neumann, R.; Khenkin, A. M. *Inorg. Chem.* **1995**, *34*, 5753.

(7) Nomiya, K.; Torii, H.; Nomura, K.; Sato, Y. *J. Chem. Soc., Dalton Trans.* **2001**, 1506.

(8) (a) Bi, L.-H.; Hussain, F.; Kortz, U.; Sadakane M.; Dickman, M. H. *Chem. Commun.* **2004**, 1420. (b) Bi, L.-H.; Kortz, U.; Keita, B.; Nadjo, L. *Dalton Trans.* **2004**, 3184. (c) Bi, L.-H.; Dickman, M. H.; Kortz, U.; Dix, I. *Chem. Commun.* **2005,** 3962.

(9) (a) Süss-Fink, G.; Plasseraud, L.; Ferrand, V.; Stoeckli-Evans, H. *Chem. Commun.* **1997**, 1657. (b) Süss-Fink, G.; Plasseraud, L.; Ferrand, V.; Stanislas, S.; Neels, A.; Stoeckli-Evans, H.; Henry, M.; Laurenczy, G.; Roulet, R. *Polyhedron* **1998**, *17*, 2817. (c) Plasseraud, L.; Stoeckli-Evans, H.; Süss-Fink, G. *Inorg. Chem. Commun.* **1999**, *2*, 344. (d) Artero, V.; Proust, A.; Herson, P.; Thouvenot, R.; Gouzerh, P. *Chem. Commun.* **2000**, 883. (e) Artero, V.; Proust, A.; Herson, P.; Gouzerh, P. *Chem.—Eur. J.* **2001**, *7*, 3901. (f) Villanneau, R.; Artero, V.; Laurencin, D.; Herson, P.; Proust, A.; Gouzerh, P. *J. Mol. Struct.* **2003**, *656*, 67. (g) Laurencin, D.; Garcia Fidalgo, E.; Villanneau, R.; Villain, F.; Herson, P.; Pacifico, J.; Stoeckli-Evans, H.; Bénard, M.; Rohmer, M.-M.; Süss-Fink, G.; Proust, A. *Chem.—Eur. J.* **2004**, *10*, 208.

(10) (a) Artero, V.; Proust, A.; Herson, P.; Villain, F.; Moulin, C. C. D.; Gouzerh, P. *J. Am. Chem.* Soc. **2003**, *125*, 11156. (b) Artero, V.; Laurencin, D.; Villanneau, R.; Thouvenot, R.; Herson, P.; Gouzerh, P.; Proust, A. *Inorg. Chem.* **2005**, *44*, 2826.

(11) Laurencin, D.; Villanneau, R.; Herson, P.; Thouvenot, R.; Jeannin, Y.; Proust, A. *Chem. Commun.* **2005**, 5524.

(12) Bi, L.-H.; Kortz, U.; Dickman, M. H.; Keita, B.; Nadjo, L. *Inorg. Chem.* **2005**, *44*, 7485.

(13) (a) Tézé, A.; Hervé, G. *Inorg. Synth.* **1990**, *27*, 88. (b) Canny, J.; Tézé, A.; Thouvenot, R.; Hervé, G. *Inorg. Chem.* **1986**, *25*, 2114.

(14) (a) Bassil, B. S.; Kortz, U.; Tigan, A. S.; Clemente-Juan, J. M.; Keita, B.; de Oliveira, P.; Nadjo, L. *Inorg. Chem.* **2005**, *44*, 9360. (b) Hussain, F.; Bassil, B. S.; Bi, L.-H.; Reicke, M.; Kortz, U. *Angew. Chem., Int. Ed.* **2004**, *43*, 3485. (c) Mialane, P.; Dolbecq, A.; Marrot, J.; Riviere, E.; Sécheresse, F. *Chem.—Eur. J.* **2005**, *11*, 1771. (d) Kim, K.-C.; Gaunt, A.; Pope, M. T. *J. Clust. Sci.* **2002**, *13*, 423.

(15) Kamata, K.; Yonehara, K.; Sumida, Y.; Yamaguchi, K.; Hikichi, S.; Mizuno, N. *Science* **2003**, *300*, 964.

(16) Nsouli, N. H.; Bassil, B. S.; Dickman, M. H.; Kortz, U.; Keita, B.; Nadjo, L. *Inorg. Chem.* **2006**, *45*, 3858.

W, 58.6 (57.8); Ru, 6.4 (6.0); Si, 0.9 (1.1); C, 4.6 (4.8); H, 1.0 (1.2). NMR of **K-1** in H_2O/D_2O at 293 K. ^{1}H: δ 5.90, 5.91, 5.93, 6.03 (all singlets). ^{13}C: δ 80.2, 80.5, 81.7, 81.8 (all singlets). ^{29}Si: δ −84.8 (see Figure SI1).

K_4[{Ru(C_6H_6)(H_2O)}{Ru(C_6H_6)}(γ-$GeW_{10}O_{36}$)]·7H_2O (K-2). A 0.27 g (0.54 mmol) sample of [Ru(C_6H_6)Cl_2]$_2$ was dissolved in 20 mL of water, followed by addition of 1.56 g (0.54 mmol) of K_8[γ-$GeW_{10}O_{36}$]·6H_2O. The pH value was adjusted to pH 2.5 by addition of 1 M HCl. This solution was heated to 80 °C for 1 h and then cooled to room temperature. The solution was filtered, and then 1.0 mL of 1.0 M CsCl was added. A small amount of orange precipitate appeared which was immediately filtered off. on the basis of the IR results, this solid seems to be a benzene−Ru(II)-containing germanotungstate, but so far, we have not been able to determine the structure of this polyanion. Then, 2.0 mL of 1.0 M KCl was added to the filtrate, which was allowed to evaporate in an open beaker at room temperature. Brown needle-shaped crystals started to appear after 1 day. Evaporation was continued until the solvent approached the solid product (yield = 0.82 g, 48%). IR of **K-2**: 3072(w), 2924(w), 2848(w), 2361(w), 2333(w), 1435(w), 948(s), 872(sh), 844(s), 795(s), 725(s), 674-(m), 611(w), 531(m), 463(m) cm^{-1}. Anal. Calcd (Found) for **K-2**: K, 5.0 (4.8); W, 58.4 (58.8); Ru, 6.4 (6.1); Ge, 2.3 (2.5); C, 4.6 (4.8); H, 0.9 (0.9). NMR of **K-2** in H_2O/D_2O at 293 K. ^{1}H: δ 5.87, 5.94, 6.04, 6.08 (all singlets). ^{13}C: δ 81.2, 81.5, 82.2, 82.3 (all singlets).

Elemental analyses were performed by ANALYTIS, Gesellschaft für Laboruntersuchungen mbH, Cologne, Germany. Infrared spectra were recorded on KBr pellets using a Nicolet Avatar spectrophotometer. All NMR spectra were recorded on a 400 MHz JEOL ECX instrument at room temperature using H_2O/D_2O as solvent. The ^{183}W NMR measurements were performed at 16.656 MHz in 10 mm tubes, and the ^{29}Si, ^{13}C, and ^{1}H spectra were recorded in 5 mm tubes at 79.425, 100.525, and 399.782 MHz, respectively. Chemical shifts are reported with respect to 2 M Na_2WO_4 for ^{183}W and to $(CH_3)_4Si$ for ^{29}Si, ^{13}C, and ^{1}H. All chemical shifts downfield of the references are reported as positive. Thermogravimetric analyses were carried out on a TA Instruments SDT Q600 thermobalance with a 100 mL/min flow of nitrogen; the temperature was ramped from 20 to 800 °C at a rate of 5 °C/min.

X-ray Crystallography. Single crystals of **K-1** and **K-2** were mounted on a Hampton cryoloop for indexing and intensity data collection at 173 K on a Bruker Kappa APEX II single-crystal diffractometer using Mo Kα radiation (λ = 0.71073 Å). Direct methods were used to solve the structures and to locate the heavy atoms (SHELXS97). Then the remaining atoms were found from successive difference maps (SHELXL97). The final cycle of refinement for **K-1**, including atomic coordinates, anisotropic thermal parameters (W, Ru, and Si atoms, as well as K1 and K2) and isotropic thermal parameters (O and C atoms, as well as K3−K5) converged at R = 0.057 and R_w = 0.140 ($I > 2\sigma(I)$). In the final difference map, the deepest hole was −3.823 e Å^{-3}, and the highest peak was 3.601 e Å^{-3}. The final cycle of refinement for **K-2**, including atomic coordinates, anisotropic thermal parameters (W, Ru, and Ge atoms), and isotropic thermal parameters (K, O, and C atoms) converged at R = 0.073 and R_w = 0.175 ($I > 2\sigma(I)$). In the final difference map, the deepest hole was −3.457 e Å^{-3}, and the highest peak was 6.112 e Å^{-3}. Routine Lorentz and polarization corrections were applied and an absorption correction was performed using the SADABS program.[17] The crystallographic data for **K-1** and **K-2** are summarized in Table 1.

(17) Sheldrick, G. M. *SADABS*; University of Göttingen: Göttingen, Germany, 1996.

Table 1. Crystal Data and Structure Refinement for K_4[{Ru(C_6H_6)(H_2O)}{Ru(C_6H_6)}(γ-$SiW_{10}O_{36}$)]·9H_2O (**K-1**) and K_4[{Ru(C_6H_6)(H_2O)}{Ru(C_6H_6)}(γ-$GeW_{10}O_{36}$)]·7H_2O (**K-2**)

	K-1	K-2
empirical formula	$C_{12}H_{32}K_4O_{46}Ru_2SiW_{10}$	$C_{12}GeH_{28}K_4O_{44}Ru_2W_{10}$
fw	3137.6	3146.1
space group	$Pmn2_1$ (No. 31)	$Pmn2_1$ (No. 31)
a (Å)	13.6702(3)	13.6684(12)
b (Å)	16.2419(4)	16.297(2)
c (Å)	12.1397(2)	12.1607(13)
vol (Å^3)	2695.38(10)	2708.9(5)
Z	2	2
temp (°C)	−100	−100
wavelength (Å)	0.710 73	0.710 73
d_{calcd} (Mg m^{-3})	3.82	3.81
abs coeff (mm^{-1})	22.22	22.59
R [$I > 2\sigma(I)$]^a	0.057	0.073
R_w (all data)^b	0.140	0.175

^{a} $R = \sum||F_o| - |F_c||/\sum|F_o|$. ^{b} $R_w = [\sum w(F_o^2 - F_c^2)^2/\sum w(F_o^2)^2]^{1/2}$.

Results and Discussion

Synthesis and Structure. The benzene−Ru(II)-supported decatungstosilicate [{Ru(C_6H_6)(H_2O)}{Ru(C_6H_6)}(γ-$SiW_{10}O_{36}$)]$^{4-}$ (**1**) and the isostructural decatungstogermanate [{Ru(C_6H_6)(H_2O)}{Ru(C_6H_6)}(γ-$GeW_{10}O_{36}$)]$^{4-}$ (**2**) were synthesized in aqueous acidic medium (pH 2.5) in a one-pot reaction of [Ru(C_6H_6)Cl_2]$_2$ with the dilacunary polyanion precursors [γ-$SiW_{10}O_{36}$]$^{8-}$ and [γ-$GeW_{10}O_{36}$],$^{8-}$ respectively. Polyanions **1** and **2** consist of a (γ-$XW_{10}O_{36}$) fragment (X = Si, Ge) to which a Ru(C_6H_6)(H_2O) group and a Ru(C_6H_6) group are coordinated resulting in an unprecedented polyanion structure with C_s symmetry (see Figures 1 and 2). Interestingly, the two benzene−Ru groups are bound at different sites and via different bonding modes to the dilacunary polyoxotungstate fragment. The Ru(C_6H_6)(H_2O) unit occupies the lacunary site of the polyanion, and it is coordinated via two Ru−O(W) bonds on one side of the lacuna; it also has a terminal water ligand. On the other hand, the Ru(C_6H_6) unit is not bound at the lacunary site but rather on the side of the polyanion, adjacent to where the Ru(C_6H_6)-(H_2O) unit is located. The Ru(C_6H_6) unit is bound via three Ru−O(W) bridges to a rectangular polyanion face composed of a cyclic W_4O_4 entity with four μ_2-oxo bridges. It appears that the vacant site of the polyanion does not allow binding of more than one Ru(C_6H_6)(H_2O) group, most likely, because of steric effects. However, the nucleophilicity of the mono-benzene−Ru-substituted (γ-$XW_{10}O_{36}$) fragment is apparently large enough to bind an additional Ru(C_6H_6) electrophile, which then coordinates to a polyanion surface which provides the best match in terms of steric and electronic parameters.

Very recently our group showed that Ru(C_6H_6) units can also be bound to trilacunary silico- and germanotungstates by isolating [(RuC_6H_6)$_2$$XW_9O_{34}$]$^{6-}$ (X = Si, Ge).[12] Interestingly, also in these polyanions two Ru(C_6H_6) groups are coordinated to the tungsten-oxo framework. Not only that, but in complete analogy to **1** and **2**, only one Ru(C_6H_6) unit is bound at the lacunary site, whereas the other one is grafted to all three μ_2-oxo bridges of the W_3O_{13} cap on the opposite side of the trilacunary Keggin unit. Nevertheless, it must be realized that the respective bonding modes of the benzene−Ru fragment at the lacunary site is rather different in [(RuC_6H_6)$_2$-

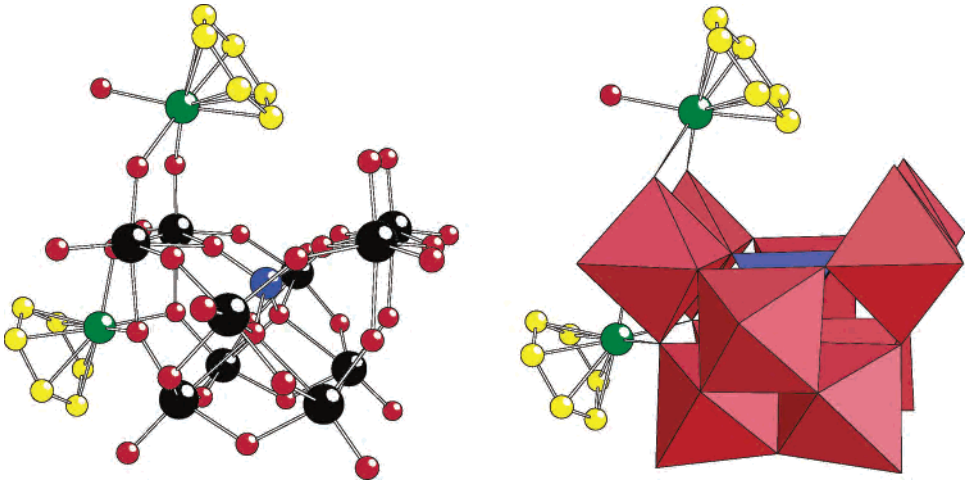

Figure 1. Ball and stick (left) and polyhedral (right) representations of $[\{Ru(C_6H_6)(H_2O)\}\{Ru(C_6H_6)\}(\gamma\text{-}SiW_{10}O_{36})]^{4-}$ (**1**) and $[\{Ru(C_6H_6)(H_2O)\}\{Ru(C_6H_6)\}(\gamma\text{-}GeW_{10}O_{36})]^{4-}$ (**2**). The balls represent tungsten (black), silicon/germanium (blue), ruthenium (green), oxygen (red), and carbon (yellow). The SiO_4/GeO_4 tetrahedron is blue and the WO_6 octahedra are red. No hydrogens are shown for clarity.

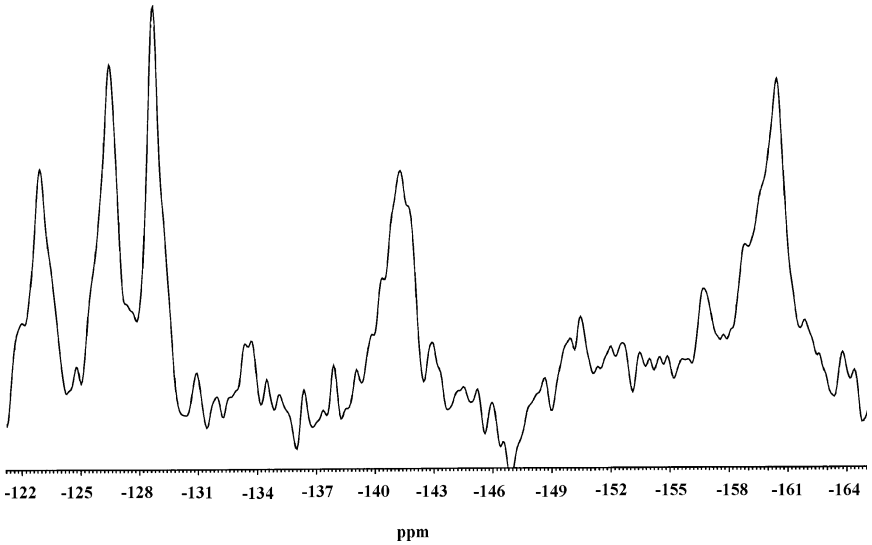

Figure 2. ^{183}W NMR spectrum of $K_4[\{Ru(C_6H_6)(H_2O)\}\{Ru(C_6H_6)\}(\gamma\text{-}GeW_{10}O_{36})]\cdot 7H_2O$ (**K-2**) in H_2O/D_2O at 293 K.

$XW_9O_{34}]^{6-}$ (three Ru−O bonds) compared to **1** and **2** (two Ru−O bonds).

Bond-valence sum calculations[18] indicate that there are no protonation sites on **1** and **2**, and therefore, the charge of the polyanions must be −4. In the solid state, the negative charge of **1** and **2** is balanced exclusively by potassium ions, which could be almost completely identified by X-ray diffraction. The results of elemental analysis confirm the chemical composition of **K-1** and **K-2**. In addition to elemental analysis, we also subjected **K-1** and **K-2** to thermogravimetric analysis, which is very useful to confirm the degree of hydration and also to evaluate the high-temperature stability of our polyanions. Our thermograms (see Figures SI2 and SI3) are very consistent with each other and also with the molecular formulas and chemical compositions of **K-1** and **K-2**. In the temperature range of 20−200 °C for **K-1** and 20−165 °C for **K-2**, we can clearly identify the loss of crystal water. Then the respective anhydrous salts are stable up to 355 (**K-1**) and 350 °C (**K-2**). At this point, weight loss occurs up to 610 (**K-1**) and 550 °C (**K-2**), but two consecutive domains can clearly be distinguished. The first region (355−405 °C for **K-1** and 350−400 °C for **K-2**) almost certainly corresponds to loss of the two benzene ligands, followed by isomerization/rearrangement/decomposition of polyanions **1** and **2**. In summary, **K-1** and **K-2** exhibit an unexpectedly high thermal stability so that heterogeneous catalysis studies for **1** and **2** are feasible up to around 400 °C.

We also performed multinuclear solution NMR on the diamagnetic polyanions **1** and **2**. For the ^{183}W NMR measurements, we redissolved solid **K-1** and **K-2** in H_2O/D_2O at room temperature, and we also added solid $LiClO_4$, LiCl, or both to increase the concentration of the solute to the maximum. For **K-1**, we could detect some signals, but we were unable to obtain spectra with a good enough signal-to-noise ratio to draw definitive conclusions. Probably, the solubility of **K-1** is too low for ^{183}W NMR. On the other hand, we were able to obtain a ^{183}W NMR spectrum for

(18) Brown, I. D.; Altermatt, D. *Acta Crystallogr.* **1985**, *B41*, 244.

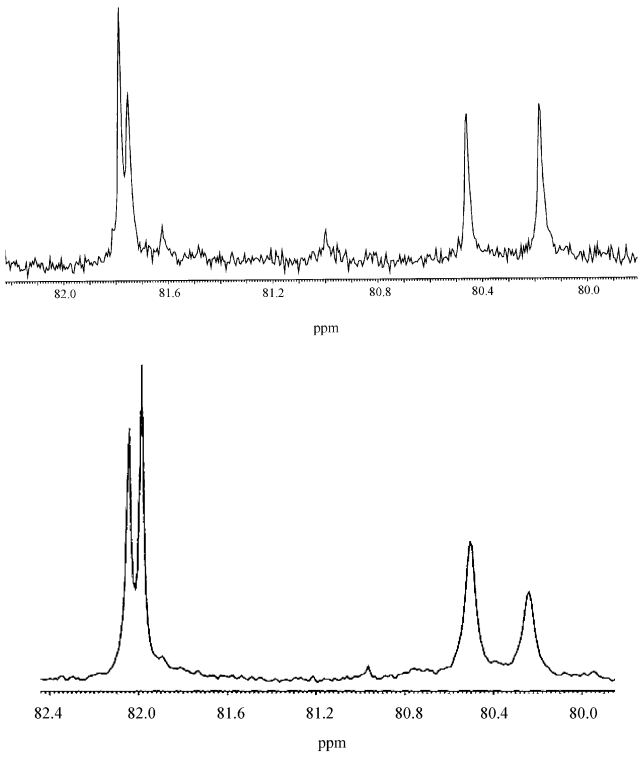

Figure 3. ^{13}C NMR spectra of $K_4[\{Ru(C_6H_6)(H_2O)\}\{Ru(C_6H_6)\}(\gamma\text{-}SiW_{10}O_{36})]\cdot 9H_2O$ (**K-1**, top) and $K_4[\{Ru(C_6H_6)(H_2O)\}\{Ru(C_6H_6)\}(\gamma\text{-}GeW_{10}O_{36})]\cdot 7H_2O$ (**K-2**, bottom) in H_2O/D_2O at 293 K.

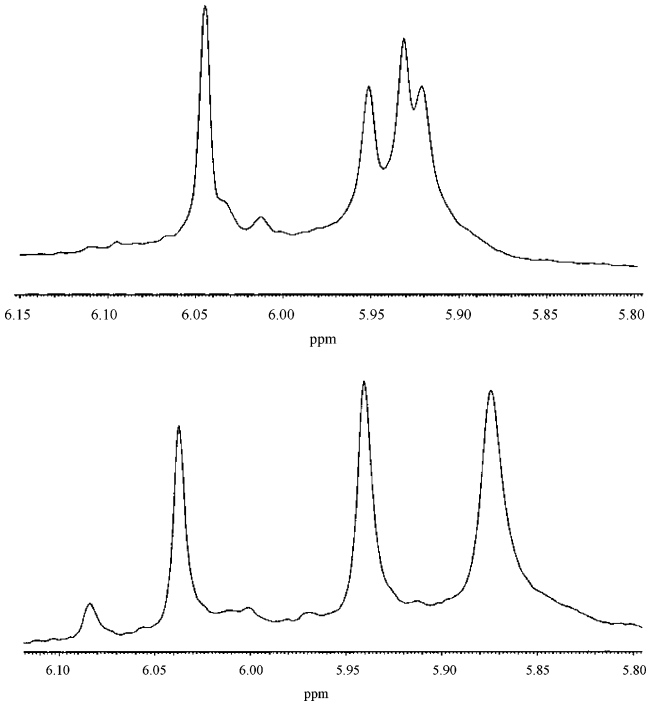

Figure 4. ^1H NMR spectra of **K-1** (top) and **K-2** (bottom) in H_2O/D_2O at 293 K.

redissolved **K-2** (see Figure 2). We see the expected 5 peaks of about equal intensity (−122.9, −126.3, −128.6, −141.5, and −160.6 ppm), which correspond to the C_s symmetry of polyanion **2** in the solid state (see Figure 1). The peaks are somewhat broader than usual, and we ascribe this to the presence of some free, paramagnetic Ru^{3+} ions, which probably originate from partial decomposition of **2** (vide infra). The ^{13}C NMR spectrum for **K-1** exhibits four peaks at 80.2, 80.5, 81.7, and 81.8 ppm, and for **K-2**, we also observe four signals at 81.2, 81.5, 82.2, and 82.3 ppm (see Figure 3). On the basis of the ^{13}C NMR studies with the precursor $[Ru(C_6H_6)Cl_2]_2$ and free benzene in the same medium, we conclude that the two downfield signals at 81.7 and 81.8 ppm correspond to **1** and those at 82.2 and 82.3 ppm to **2**. In fact, we expect only one signal for all six carbons of C_6H_6 because of the fast rotation of the benzene unit around the Ru−(η^6-C_6H_6) bond axis. This result is in complete agreement with our observations for the related $[(RuC_6H_6)_2SiW_9O_{34}]^{6-}$ and $[(RuC_6H_6)_2GeW_9O_{34}]$.[6−12] It can also be noticed that the two downfield peaks in the ^{13}C NMR spectra of **1** and **2** are considerably narrower than the respective two upfield peaks. We believe that the latter originate from free benzene−Ru fragments which have broken off polyanions **1** and **2**. The peak broadening is most likely caused by the presence of paramagnetic Ru^{3+} centers. In complete agreement with the ^{13}C spectrum, the ^1H NMR spectrum for **K-1** also exhibits four signals (see Figure 4). However, in this case, the assignment is more complicated than for ^{13}C because the signals are much closer together (especially the three upfield peaks which partially overlap). Nevertheless, we can clearly identify the peak maxima at 5.90, 5.91, 5.93, and 6.03 ppm. For **K-2**, we also observe four peaks at 5.87, 5.94, 6.04, and 6.08 ppm, but the latter signal has a significantly lower intensity than the other three (see Figure 4). In analogy with ^{13}C NMR, we expect two signals in each ^1H NMR spectrum to originate from **1** and **2**, whereas the other two peaks originate, most likely, from the same broken-off benzene−Ru fragments as above. However, we do not feel confident about an assignment of the peaks, although we also performed ^1H NMR studies with the precursor $[Ru(C_6H_6)Cl_2]_2$ and free benzene in the same medium. Finally, the ^{29}Si NMR of **K-1** shows the expected singlet at −84.8 ppm (see Figure S1). We also did ^1H and ^{13}C NMR measurements on **K-1** and **K-2** in very acidic 1 M HCl (pH 0) medium, the same solvent used for the electrochemistry experiments (vide infra). Using these conditions, we always discovered significant amounts of free benzene in solution. This is very contrary to our observations in the pH range of 2.5−6, where no significant loss of benzene was observed. It appears that, with these conditions, loss of the entire benzene−Ru fragment is more pronounced, whereas in very acidic medium, only the organic ligand is exchanged. These results are in full agreement with our electrochemistry data.

The synthesis of **1** and **2** was accomplished by a one-pot reaction of $[\gamma\text{-}XW_{10}O_{36}]^{8-}$ (X = Si, Ge) and $[Ru(C_6H_6)Cl_2]_2$ in an equimolar ratio in aqueous acidic medium (pH 2.5) at 80 °C. This indicates that the dimeric Ru precursor is hydrolyzed at such conditions, providing the reactive mononuclear electrophile in situ. We also performed reactions of $[Ru(C_6H_6)Cl_2]_2$ and $[\gamma\text{-}XW_{10}O_{36}]^{8-}$ in ratios larger than 1:1 (e.g., 2:1), but we always observed formation of **1** and **2** only. This observation suggests that for steric and electronic reasons not more than two (RuC_6H_6) groups can be attached

to the dilacunary γ-Keggin core. The synthesis medium (pH 2.5) for **1** and **2** is very different from that of our reported $[(RuC_6H_6)_2XW_9O_{34}]^{6-}$ (X = Si, Ge),[12] which were synthesized at pH 6.0. We tested if **1** and **2** could also be synthesized at pH 6.0, but we could not isolate **1** or **2** using the same conditions as those for the synthesis of $[(RuC_6H_6)_2XW_9O_{34}]^{6-}$ (X = Si, Ge).

Interestingly, our results on **1**, **2**, and $[(RuC_6H_6)_2XW_9O_{34}]^{6-}$ (X = Si, Ge) indicate that in all cases the highly reactive di- and trilacunary Keggin species, $[\gamma\text{-}XW_{10}O_{36}]^{8-}$ and $[\alpha\text{-}XW_9O_{34}]^{10-}$ (X = Si, Ge), are stabilized by coordination of two benzene−Ru fragments, so that isomerization to other tungsten-oxo fragments is inhibited.

Electrochemistry. General methods, materials, and electrochemical procedures were described previously.[8b,19] The stability of **1** and **2** was assessed by monitoring their UV−vis spectra and their cyclic voltammograms in 1 M HCl (pH 0), a medium suitable for testing selected electrocatalytic processes. The reproducibility of the spectra with respect to absorption band intensities and wavelength locations and the reproducibility of cyclic voltammograms indicate that the two complexes are stable in this medium. It is worth noting that the stability of **1** in pH 0 medium must be contrasted with that of its lacunary precursor $[\gamma\text{-}SiW_{10}O_{36}]^{8-}$ in pH < 1 media.[13a] The lacunary precursor of **2** is $[\gamma\text{-}GeW_{10}O_{36}]^{8-}$, and we discovered that it decomposes more slowly in a pH 0 medium than its Si analogue. The electrochemistry of both lacunary precursor species is known.[13a,16] In general, we observed analogous electrochemical behavior for **1** and **2**. Therefore, a complete report will be given only for **1** complemented by some unique features for **2**. For clarity and ease of comparison, the respective electrochemical behavior of the W and Ru centers within **1** and **2** will be described separately. Figure 5A shows the first two waves corresponding to the reduction of the W centers of **1** in 1 M HCl (pH 0). The second wave is composite with two reduction peaks associated with only one clearly visible oxidation process. The observed splitting of the second wave should be associated with the acid−base properties of the reduced forms of **1**. In support of this assumption, it would be interesting to study acidity effects on the cyclic voltammograms. Unfortunately, the pH stability domain of **1** and **2** is narrow, precluding a detailed electrochemical study as a function of medium acidity. However, some general electrochemistry trends are known with respect to the behavior of the W waves of plenary and lacunary Keggin-type POMs with Si and Ge heteroatoms. These trends are also known for transition metal-containing derivatives, in particular Fe^{3+}- and Ru^{2+}-substituted POMs.[8b,20] First, the potential locations of these W waves are influenced by changing the hetero group. Second, at the very least, the first two W waves appear at less negative potentials in Ge−POMs than in the corresponding Si−POMs.[8b,20] With all other things being equal except for the heteroatoms, this intrinsic behavior is paralleled by the basicity of the respective reduced species.

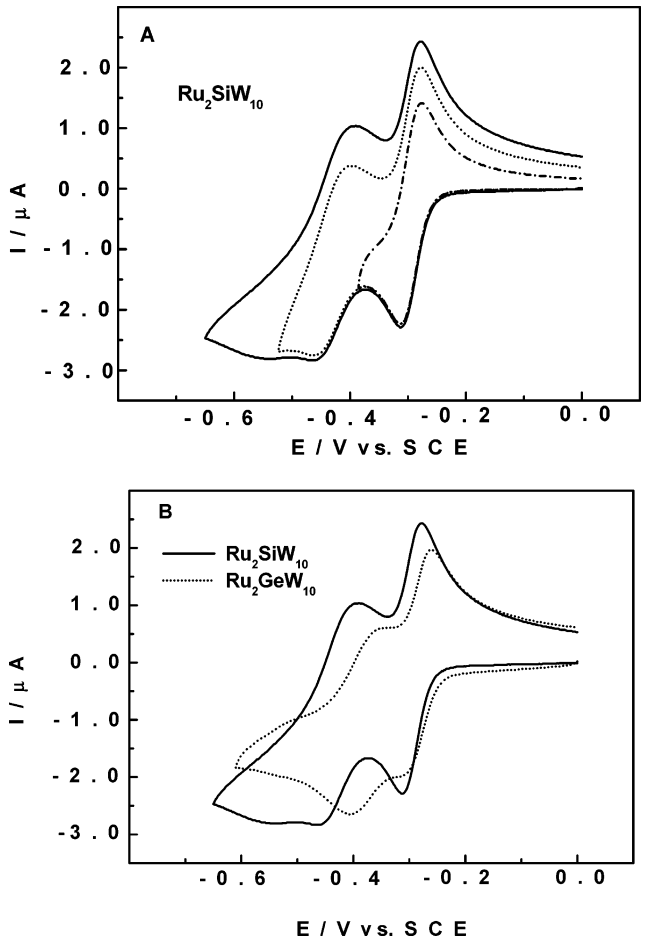

Figure 5. Cyclic voltammograms of 2×10^{-4} M **1** and **2** in 1 M HCl (pH 0) medium. The working electrode was glassy carbon and the reference electrode was SCE. The scan rate was 10 mV s^{-1}. (A) The voltammetric pattern for **1** is restricted to the W redox processes. Three cathodic potential limits were selected to highlight the various steps. (B) Superimposed voltammetric patterns for **1** and **2**, restricted to the W redox processes.

In the present context, such reasoning led us to consider that differences in the cyclic voltammograms reflect differences in the acid−base properties of the reduced species. A simple rule is that the addition of electrons increases the basicity of the reduced species compared to that of the corresponding oxidized form. However, a few examples of p*K* inversion are also known in POM electrochemistry. Controlled potential electrolysis at pH 0, on the first W wave of **1** at − 0.350 V vs SCE consumes 2.3 electrons per molecule, a value slightly larger than the expected two electrons, on the basis of the behavior of the lacunary precursors.[13a] Complete reoxidation was achieved with recovery of two electrons per molecule. Such observation is not uncommon in Ru-substituted polyoxometalates and has in fact been encountered previously for $[Ru(dmso)_3(H_2O)XW_{11}O_{39}]^{6-}$ (X = Ge, Si)[8b] and $[Ru^{III}(H_2O)PW_{11}O_{39}]^{4-}$.[21] For the latter, the electrocatalytic proton reduction process triggered by the reduced form of the polyanion (prepared on the first W wave) was so important that no coulometry was possible. It must be concluded that the rate of the electrocatalytic process is modest for **1**, as observed previously for $[Ru(dmso)_3(H_2O)XW_{11}O_{39}]^{6-}$ (X = Ge, Si).[8b]

(19) Keita, B.; Girard, F.; Nadjo, L.; Contant, R.; Canny, J.; Richet, M. *J. Electroanal. Chem.* **1999**, *478*, 76.
(20) Toth, J. E.; Anson, F. C. *J. Electroanal. Chem.* **1988**, *256*, 361.

Figure 5B shows a superposition of the voltammetric patterns for **1** and **2**. The potential locations of the two W waves are closer to each other for **2** than for **1**. The main voltammetric characteristics for the first two waves of **1** and **2** are gathered in the Supporting Information (Table SI1). The formal potential for the first W wave of **2** is located at a slightly more positive potential than that of **1**. In contrast, the second W wave of **2** is distinctly more positive than that of **1**, a feature that might be traced to a difference in the acid−base properties of the reduced forms of the two complexes. At variance with the behavior observed for **1**, almost no splitting was observed for the second W wave of **2**. For **1**, the anodic-to-cathodic peak potential difference, ΔE_p, value of 0.032 V is expected on theoretical grounds for a two-electron process, while the value of 0.070 V underscores the tendency of the second wave to split into one-electron processes. The corresponding ΔE_p values for **2** remain constant, a behavior that could be expected from the lack of splitting of the second W wave. Finally, controlled potential electrolysis at pH 0, on the first W wave of **2** at −0.325 V vs SCE consumes 2.0 electrons per molecule. Of note is the absence of the electrocatalytic process for **1**, a behavior that can be attributed to the slightly more positive location of the first W wave of **2**. Complete reoxidation was also achieved here, with recovery of two electrons per molecule as expected from the electrochemistry of the lacunary $[\gamma\text{-}GeW_{10}O_{36}]^{8-}$.[16] This observation allows for an easier study of other electrocatalytic reduction processes with **2**.

These observations can be compared with those for $[Ru(dmso)_3(H_2O)XW_{11}O_{39}]^{6-}$ (X = Ge, Si).[8b] For these Ru-(dmso)-containing species, both W waves are distinctly more positive in the Ge- than in the Si-POM. In contrast, for **1** and **2**, only the second waves show substantially different potential locations. The comparison with $[(RuC_6H_6)_2XW_9O_{34}]^{6-}$ (X = Si, Ge)[12] is less straightforward, probably because of the acid−base properties.

With **1** as the main illustrative example, Figure 6A shows a typical voltammetric pattern in HCl 1 M (pH 0) medium where the potential domain is extended from the location of the previously described W waves to 1.3 V vs SCE. In addition to the W waves, a large intensity oxidation wave was observed, which peaks at 1.260 V vs SCE. This wave has no cathodic counterpart upon potential reversal. Restricting the potential domain to the positive region indicated the perfect reproducibility of the pattern observed in this domain, see Figure 6A. In Figure 6B, this voltammetric pattern is compared with that obtained when the positive potential limit was extended from 1.3 to 1.5 V. Just positive of the peak observed at 1.260 V, a very large intensity oxidation current begins, which is associated, upon potential reversal, with a broad cathodic counterpart peaking at 0.470 V vs SCE. Analogous phenomena were observed for **2**: (i) a well-behaved oxidation wave peaks at 1.330 V with no associated cathodic counterpart, and (ii) a cathodic counterpart with a peak at 0.390 V appears when the positive potential limit

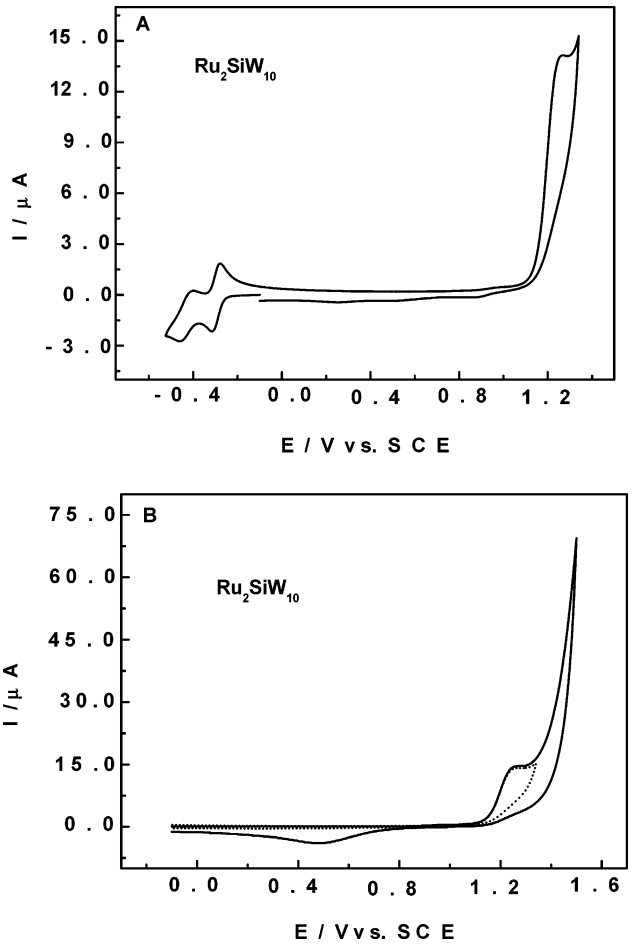

Figure 6. Cyclic voltammograms of 2×10^{-4} M **1** in 1 M HCl (pH 0) medium. The working electrode was glassy carbon and the reference electrode was SCE. The scan rate was 10 mV s^{-1}. (A) The voltammetric pattern for **1** shows both anodic and cathodic processes. (B) The voltammetric pattern for **1** is restricted to anodic processes and shows the effect of varying the positive potential limit.

was driven beyond 1.5 V. For both complexes, a comparison of the current intensities of these waves with those of the W-centers leads to the conclusion that they should be assigned, respectively, to the polyanion-assisted oxidation of the benzene−Ru fragment and the solvent. Except for the benzene−Ru moieties, there are no other oxidizable centers in **1** and **2**. Cyclic voltammetry demonstrates unambiguously that **1** and **2** do not collapse. Taking into account this observation and the current intensity of the observed oxidation wave, we have to consider both possibilities: oxidation of the benzene−Ru fragment or the solvent.

Careful examination of Figure 6 reveals the presence of a redox pattern just negative of the benzene−Ru oxidation during the ongoing positive potential scan. Figure 7A shows this wave on an appropriate scale. Its formal potential is $E^{\circ\prime} = 0.933$ V, and the anodic to cathodic peak potential difference, ΔE_p, is 0.114 V. The corresponding parameters for **2** are $E^{\circ\prime} = 0.934$ V and $\Delta E_p = 0.148$ V, respectively. Unambiguous assignment of this wave to the oxidation and re-reduction of the Ru centers grafted to **1** and **2** stems from the comparison of the observed pattern with that obtained from a sample of $[Ru(C_6H_6)Cl_2]_2$ (see Figure SI4). The formal potential for this process is $E^{\circ\prime} = 0.923$ V, with an

(21) Rong, C.; Pope, M. T. *J. Am. Chem. Soc.* **1992**, *114*, 2932.

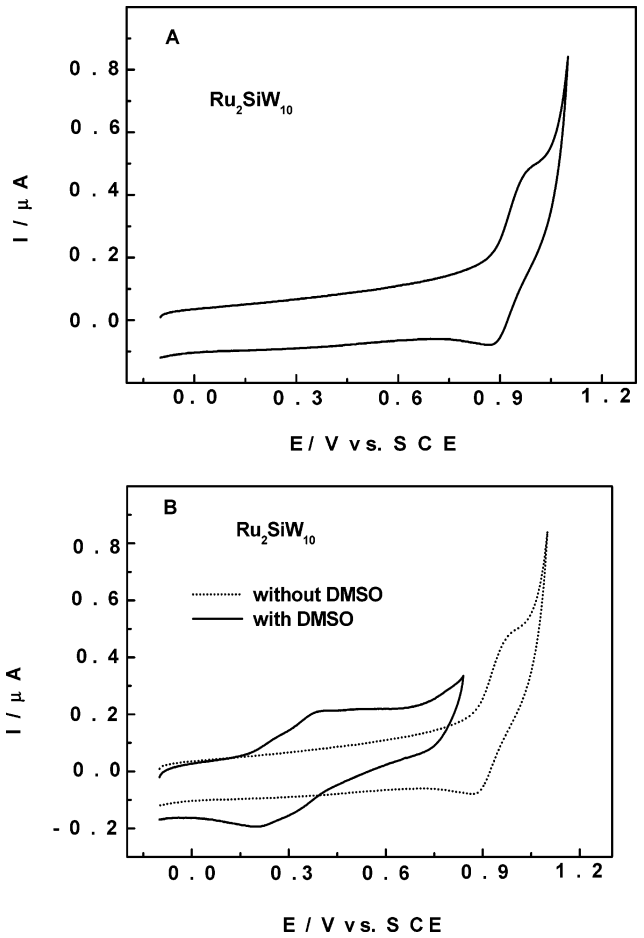

Figure 7. Cyclic voltammograms of 2×10^{-4} M **1** in 1 M HCl (pH 0) medium. The working electrode was glassy carbon and the reference electrode was SCE. The scan rate was 10 mV s^{-1}. (A) The voltammetric pattern for **1** is restricted to the redox processes of the Ru center. (B) The voltammetric patterns for **1** are restricted to the redox processes of the Ru center with and without addition of dmso.

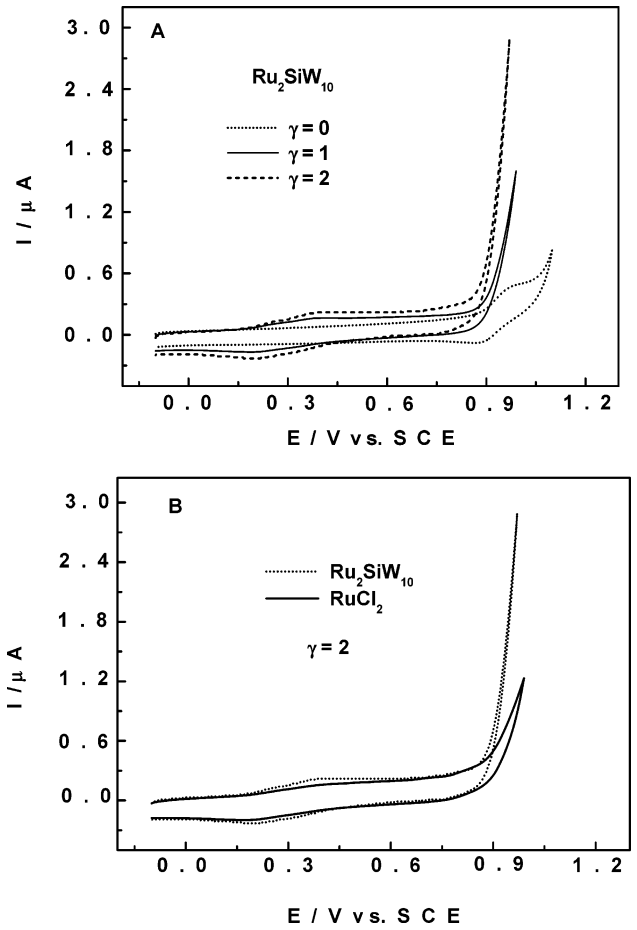

Figure 8. Cyclic voltammograms for the electrocatalytic oxidation of dmso with 2×10^{-4} M electrocatalyst in 1 M HCl (pH 0) medium. The working electrode was glassy carbon and the reference electrode was SCE. The scan rate was 10 mV s^{-1}. (A) The electrocatalyst is **1**. (B) A comparison of the two electrocatalysts **1** and $[Ru(C_6H_6)Cl_2]_2$. The excess parameter γ is defined as the concentration ratio of dmso to the polyanion ($\gamma = C_{dmso}/C_{POM}$).

anodic-to-cathodic peak potential difference, ΔE_p, of 0.175 V. Because of the presence of different ligands on Ru, these values can be compared favorably with those obtained for **1** and **2**. This identification opens the way for studying electrocatalytic processes that might be triggered by the Ru center.

Electrocatalysis. In this work, our attention was focused on the possible electrocatalytic oxidation of dmso in the presence of **1** and **2**. We discovered that both polyanions display analogous behavior. Upon addition of dmso to a solution of **1**, a ligand displacement takes place. Figure 7B shows the Ru wave in superposition before and after the addition of dmso to the solution of **1**. A new wave appears, which is substantially shifted in the negative potential direction compared to the former Ru wave. This new wave is composite and can be considered to be composed of two closely spaced waves with the following characteristics: $E_1^{\circ\prime} = 0.235$ V and $\Delta E_{p1} = 0.070$ V and $E_2^{\circ\prime} = 0.360$ V and $\Delta E_{p2} = 0.060$ V. Analogously, ligand substitution was observed upon the addition of dmso to a solution of $[Ru(C_6H_6)Cl_2]_2$ with a concomitant shift of the Ru wave in the negative potential direction. The pattern is drawn out with an oxidation peak and a reduction peak located at 0.420 and 0.170 V, respectively. We wondered if the cyclic voltammogram modifications indicate ligand substitution on the benzene−Ru moieties or complete loss of these organometallic fragments from the POM framework. In this regard, we discovered that the W waves are not affected by the addition of dmso to solutions of **1** and **2**, neither their current intensities nor their potential locations, even after several hours of standing. This observation is not in agreement with loss of entire benzene−Ru units from the Keggin core. As a matter of fact, removal of the benzene−Ru moieties from the POM framework would leave the lacunary decatungstates free in solution. The silicon precursor -$[\gamma SiW_{10}O_{36}]^{8-}$ has been studied previously by Tézé and Hervé[13a] and is known to be unstable in the pH 0 (1 M HCl) medium used for the present experiment (unless small amounts of dmso have a large stabilizing effect, but this hypothesis was checked experimentally and shown to be incorrect). As a consequence, the expected rearrangement of these dilacunary POMs (most likely to mono- and nonlacunary Keggin derivatives) in solution cannot leave the W waves of **1** and **2** unchanged. In contrast, benzene substitution is not expected to influence the W waves significantly, which is fully compatible with our observations. It should be interesting to determine which of the two benzene ligands is actually replaced, but this

problem is beyond the scope of this paper. These observations parallel the previously described ligand substitution for the aqua ligand in ruthenium-substituted heteropolytungstates.[21,22]

Figure 8A shows the voltammetric patterns observed in the absence of dmso and for two different dmso concentrations in superposition. The excess parameter, γ, is defined as the ratio of the concentration of dmso to that of the polyanion ($\gamma = C_{dmso}/C_{POM}$). A large current increase appears to start slightly negative of the former Ru wave, with the negative shift increasing with the value of γ. This wave features the electrocatalytic oxidation of dmso. Second-order rate constants of 2.30×10^3 M^{-1} $s^{-1}$and 1.50×10^3 M^{-1} s^{-1} were determined by double potential step chronocoulometry for **1** and **2**, respectively. The electrocatalytic efficiencies of **1** and $[Ru(C_6H_6)Cl_2]_2$ for the electrocatalytic oxidation of dmso are compared in Figure 8B for an excess parameter $\gamma = 2$. It can be noticed that **1** is the better catalyst. Finally, the current scale sensitivity was decreased so that, in analogy to Figure 6B, the positive potential limit could be extended to 1.5 V. A very large current intensity electrocatalytic wave was observed starting just negative of the former benzene−Ru oxidation wave and peaking roughly at 1.350 V (Figure SI5). In short, two observations support our interpretation of the influence of dmso addition to solutions of **1** and **2**. First, the Ru-centered oxidation is shifted in the negative potential direction and becomes composite. Second, the solvent limit is also displaced in the negative potential direction, and the catalytic current intensity depends on the excess of added dmso. These two observations are associated with ligand substitution on the Ru centers accompanied by efficient catalytic oxidation of dmso. The catalytic abilities of **1**, **2**, and $[Ru(benzene)Cl_2]_2$ are compared and are in favor of the POMs. To our knowledge, this observation constitutes the only example of electrocatalytic dmso oxidation, in addition to the work of Rong and Pope on the same process using $[Ru^{III}(H_2O)PW_{11}O_{39}]^{4-}$.[21]

Conclusions

We have synthesized and structurally characterized two novel organometallic Ru^{II}-supported decatungstates. The monomeric polyanions $[\{Ru(C_6H_6)(H_2O)\}\{Ru(C_6H_6)\}(\gamma\text{-}SiW_{10}O_{36})]^{4-}$ (**1**) and the isostructural germanium analogue $[\{Ru(C_6H_6)(H_2O)\}\{Ru(C_6H_6)\}(\gamma\text{-}GeW_{10}O_{36})]^{4-}$ (**2**) consist of a $Ru(C_6H_6)(H_2O)$ and a $Ru(C_6H_6)$ group linked to a dilacunary ($XW_{10}O_{36}$) Keggin fragment at different sites resulting in an assembly with idealized C_s symmetry. The $Ru(C_6H_6)(H_2O)$ group is bound at the vacant polyanion site via two Ru−O(W) bonds and a terminal water molecule, whereas the (RuC_6H_6) group is grafted on the side via three Ru−O(W) bonds. We have demonstrated that the in situ formed, dicationic (RuC_6H_6) fragment represents a highly reactive electrophile which binds instantaneously to the dilacunary Keggin-type heteropolyanion $[\gamma\text{-}XW_{10}O_{36}]^{8-}$. The fact that the γ-Keggin fragment is preserved in **1** deserves emphasis because $[\gamma\text{-}SiW_{10}O_{36}]^{8-}$ is prone to rearrangement, rotational isomerization, and loss/gain of tungsten when reacted with d-block metal ions in acidic aqueous medium.[14a−c] In complete analogy to our recently reported $[(RuC_6H_6)_2XW_9O_{34}]^{6-}$ (X = Si, Ge), two (RuC_6H_6) fragments are grafted to the Keggin unit. Polyanions **1** and **2** represent the first examples of dilacunary tungstosilicates and -germanates functionalized by organo-Ru groups. Polyanions **1** and **2** may be considered to be "semilacunary" species, because two of the four tungsten centers at the lacunary site are not involved in bonding to the $Ru(C_6H_6)(H_2O)$ group. This could be of major interest for catalytic applications of **1** and **2** (e.g., binding of substrate, oxidant, or both). In summary, polyanions **1** and **2** exhibit unprecedented and highly interesting features in the area of organo-ruthenium-containing polyoxometalates.

Electrochemistry studies on **1** and **2** have demonstrated that the central heteroatom X (Si, Ge) influences mainly the reduction potentials of the second W waves, thus indicating a variation in acid−base properties of the reduced forms of **1** and **2**. Thus, the second W wave for **1** is split, while that of **2** is not. On the oxidation side, a comparison of the electrochemical behavior of **1** and **2** with those of the precursor reagent $[Ru(C_6H_6)Cl_2]_2$ was helpful. It appears that a chemically reversible wave features the redox behavior of the Ru center. Electrocatalytic oxidation of the benzene−Ru assembly, followed by that of the electrolyte is another feature common to the three species, **1**, **2**, and $[Ru(C_6H_6)Cl_2]_2$. Ligand substitution with concomitant negative potential shift of the voltammetric pattern associated with the Ru center was observed upon addition of dmso. All observations together confirm the interpretation given for the observed electrocatalytic oxidation waves in the absence of dsmo.

Acknowledgment. U.K. thanks the International University Bremen and the German Science Foundation (DFG, Grant KO 2288/4-1) for research support. B.K. and L.N. thank the CNRS (UMR 8000) and the Université Paris-Sud XI. Figure 1 was generated by Diamond, version 3.1a (copyright Crystal Impact GbR).

Supporting Information Available: Figure SI1 showing the ^{29}Si NMR spectrum of **K-1** in H_2O/D_2O at 293 K, Figures SI2 and SI3 showing the thermograms of **K-1** and **K-2**, respectively, Figure SI4 showing the voltammetric pattern for $[Ru(C_6H_6)Cl_2]_2$ restricted to anodic processes and showing the effect of varying the positive potential limit, Figure SI5 showing cyclic voltammograms highlighting the electrocatalytic oxidation of dmso with 2×10^{-4} M **1** in 1 M HCl (pH 0) medium, Table SI1 showing the main voltammetric characteristics of the first two W waves for **1** and **2** in 1 M HCl (pH 0) medium, and complete X-ray crystallographic data for **K-1** and **K-2** (CIF format). This material is available free of charge via the Internet at http://pubs.acs.org.

IC0606835

(22) Bart, J. C.; Anson, F. C. *J. Electroanal. Chem.* **1995**, *390*, 11.